Synthetic Metals 195 (2014) 110–116

Contents lists available at ScienceDirect

Synthetic Metals

journal homepage: www.elsevier.com/locate/synmet

Structural, absorption and dispersion characteristics of nanocrystalline copper tetraphenyl porphyrin thin films

M.M. El-Nahass [a], A.A.M. Farag [a,*], Mossad El-Metwally [b], F.S.H. Abu-Samaha [c], Eman Elesh [b]

[a] Thin Film Laboratory, Department of Physics, Faculty of Education, Ain Shams University, Roxy, 11757 Cairo, Egypt
[b] Department of Physics, Faculty of Science, Port Said University, Port Said, Egypt
[c] Department of Physics & Mathematical Engineering, Faculty of Engineering, Port Said University, 42523 Port Said, Egypt

ARTICLE INFO

Article history:
Received 15 February 2014
Accepted 14 May 2014

Keywords:
CuTPP thin film
Energy gap
Dispersion parameters

ABSTRACT

Thin films of tetraphenyl porphyrin (CuTPP) were prepared by thermal evaporation technique under vacuum. The surface morphology and crystalline structural characteristics of CuTPP were achieved by atomic force microscopy (AFM). The crystalline structure of CuTPP thin films was investigated by using X-ray diffraction. The average crystallite size, D, was calculated using the modified Scherrer's equation. Optical constants (refractive index, n, and absorption index, k) of CuTPP films were estimated by using spectrophotometric measurements of transmittance and reflectance in the spectral range from 200 to 2500 nm.

The optical constants of CuTPP are independent of film thickness in the thickness range 400–1270 nm. The dependence of absorption coefficient on the photon energy was determined and the analysis of the result showed that the optical transition in CuTPP films is allowed and indirect. The onset and optical energy gap for are 1.80 and 2.30 eV, respectively. The UV–vis absorption spectrum was analyzed in terms of both molecular orbital and band theories. The optical dispersion parameters of CuTPP thin films such as oscillator energy, E_o, dispersion energy, E_d, the lattice dielectric constant, ε_L, the high frequency dielectric constant, ε_∞, and the ratio of the free charge carrier concentration to the effective mass, N/m^* were investigated. Moreover, third order nonlinear susceptibility, $\chi^{(3)}$ of CuTPP films was also considered.

1. Introduction

Organic semiconducting materials are of particular interest, since they possess advantageous electrical, optical, optoelectronic and processing properties for design and fabrication of novel class of the semiconductor-based devices such as diodes, photovoltaic devices [1,2]. These materials have advantages of low cost, ease of processing, and the ability to modify their structure to obtain the desired electrical and optical characteristics when compared with conventional inorganic semiconductors [1–4].

Organic molecules that are colored contain delocalised electrons spread over a number of atoms is known as conjugated systems [5]. The π-conjugated electron system has all the essential electronic features of organic materials: light absorption and emission, charge generation and transport [6,7].

Porphyrin dyes are a class of conjugated macrocyclic compounds in which four pyrrole rings are linked to each other in cyclic fashion through meso-carbon bridges [6]. There is currently considerable concern about photoprocesses porphyrins, metalloporphyrins and related compounds due to the applicability of these molecules in playing an essential function in many biological processes; oxygen transport to photosynthesis, catalysis to pigmentation changes, laser sciences optoelectronic techniques and electronic devices [6–8].

Porphyrins and other metalloporphyrins thin films can easily be prepared by chemical or physical methods. These methods include thermal evaporation, vapor deposition, spin coating and Langmuir Blodgett (LB) deposition techniques [6,9,10].

As an extension for studying the family of porphyrin compounds by our scientific group and the little information in the literature concerning the optical characterization of CuTPP films confirms the significance of this investigation. Moreover, to the best of our knowledge there is no thorough study of its optical properties, as reported here. Therefore, the objective of this study is to investigate the structural and optical properties of thermally evaporated thin

* Corresponding author. Tel.: +20 0233518705.
E-mail address: alaafaragg@yahoo.com (A.A.M. Farag).

http://dx.doi.org/10.1016/j.synthmet.2014.05.013
0379-6779/

Table 1
AFM parameters of CuTPP film using XEI software.

Statistics value	Mean radius (nm)	Surface area (μm^2)	Volume (nm^3)	Roughness (nm)
Average	80	0.025	3.74×10^6	1.421
Standard deviation	29	0.017	2.53×10^6	0.43

films of CuTPP including the absorption and dispersion characteristics refractive over the spectral range 200–2500 nm, and check the effect of thickness on their structural, morphological and optical properties.

2. Experimental details

CuTPP was purchased from Aldrich Chem Co. and was used as received without any further purification. The different thicknesses of CuTPP thin films are prepared by conventional thermal evaporation technique, using a high vacuum coating unit (Edwards Co. model E306A, England), under a pressure of about 4×10^{-5} Torr and the rate of deposition (2.5 nm/s). The evaporation rate is controlled by quartz crystal monitor (FTM4, Edwards). The glass and quartz optical flat substrate was used for structure and optical measurements respectively.

Surface morphology of nanocrystalline CuTPP films was studied using atomic force microscope (AFM, WET-SPM-9500-J3, Shimadzu, Japan).

The crystal structure of the different thickness was investigated by using a Philips X-ray diffractometer (model X' pert) with utilized monochromatic Cu K_α radiation ($\lambda = 1.5418$ Å).

The transmission electron microscope model (TEM) JEOL JEM - 123 has been used for investigate the crystalline structure of CuTPP thin film. JASCO spectrophotometer, model V-570 UV–VIS–NIR, was used to measure the optical transmittance (T), and reflectance (R) of different thickness of CuTPP thin films in the range of wavelength 250–2500 nm.

The refractive index, n, the absorption index, k, and the absorption coefficient, α, can be calculated by using the following equation [4,8]:

$$\alpha = \frac{1}{d} \ln \left[\frac{(1-R)^2}{2T} + \sqrt{R^2 + \frac{(1-R)^4}{4T^2}} \right] \quad (1)$$

$$k = \frac{\alpha \lambda}{4\pi} \quad (2)$$

$$n = \left(\frac{1+R}{1-R} + \sqrt{\frac{4R^2}{(1-R)^2} - k^2} \right) \quad (3)$$

3. Results and discussion

3.1. Surface morphology and crystalline structure characterization

2-D and 3-D atomic force microscope (AFM) images of CuTPP films are shown in Fig. 1(a) and (b) for studying the surface morphology and surface roughness. Accompanied XEI software was used for the data processing and analyzing of the extracted parameters such as the average values and the standard deviations of roughness and particles sizes. The average and standard deviation values of the mean radius, surface area values roughness and the particles sizes are calculated and listed in Table 1. The AFM results indicate that a nearly homogeneous deposition is obtained for films, except the upper corner of the film, under the thermal evaporation conditions. A rough characteristic for the film surface is favorable for solar cell applications because the rough surface will trap more light [11].

XRD patterns of CuTPP film onto glass substrates are shown in Fig. 2. Miller indices of the main preferred orientation peaks along (0 2 0) and (1 2 1) are matched with those published before by El-Nahass et al. [12]. The obtained patterns indicate that the CuTPP film is partially crystallized and no change on the position of the diffraction peaks. The analysis also indicates that CuTPP has the triclinic form with space group ($P-1$) and lattice constants of $a = 12.905$ Å, $b = 20.994$ Å and $c = 9.82$ Å.

Moreover, the diffracted peaks are observed to be broad at half maximum. Broadening of diffracted peaks is mainly due to lattice microstrain and smaller crystallite size. The average crystallite size, D, was calculated using the modified Scherrer's equation [13]:

$$D = \frac{K\lambda}{\sqrt{\beta_1^2 - \beta_2^2 \cos\theta}} \quad (4)$$

where λ is the X-ray wavelength, K is a constant (~0.94), β_1 and β_2 are the width at half maxima of the broadened peaks of CuTPP and a

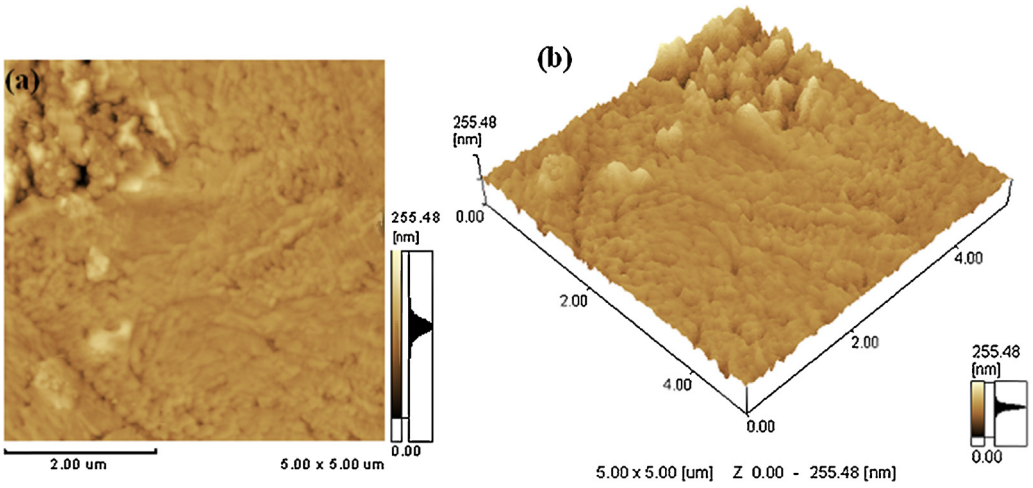

Fig. 1. AFM images of surface topography of CuTPP thin film (a) 2-D image, (b) 3-D image.

Table 2
Comparison between d_{hkl} obtained from XRD and SAED for CuTPP film.

No.	$d_{measured}$ (XRD)	$d_{calculated}$ (SAED)	($h\,k\,l$)
1	10.1	9.3	(0 2 0)
2	7.1	6.1	(1 2 1)

standard silicon crystal, respectively. The use of silicon defect free crystal measures the instrumental broadening. The low scanning rate of the 2θ and neglecting the micro-strain of the nonthermal stressed films enabled us to calculate the crystallite size using Eq. (4). Fig. 2 also shows the Gaussian fit of the peaks of XRD for CuTPP film. As a result, the mean crystallite size can be calculated to be ~60 nm.

The crystalline structure of CuTPP film was also checked using the transmission electron microscopy (TEM). Fig. 3(a) and (b) shows TEM micrograph for the crystallite size and selected area electron diffraction of CuTPP film, respectively. The average crystallite size is ~8 nm, which is lower than those obtained from XRD results. This may be attributed from the neglecting the contribution of lattice microstrain for calculating mean crystallite using XRD. The selected area electron diffraction (SAED) of the CuTPP film presents information about material type, complexity and cell parameter determination. The SAED image in Fig. 3b shows high packing density assembly and some spots are observed that can be attributed to the mosaic structure of CuTPP film. The calculated d-values from (SAED) patterns are in agreement with X-ray diffraction patterns results as tabulated in Table 2.

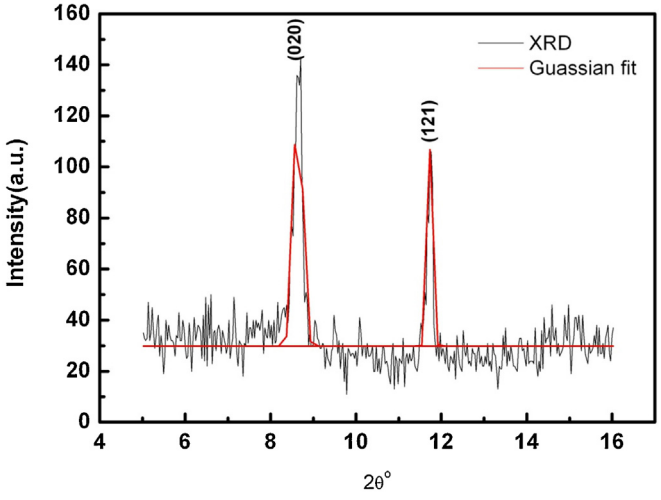

Fig. 2. XRD pattern of as deposited CuTPP film.

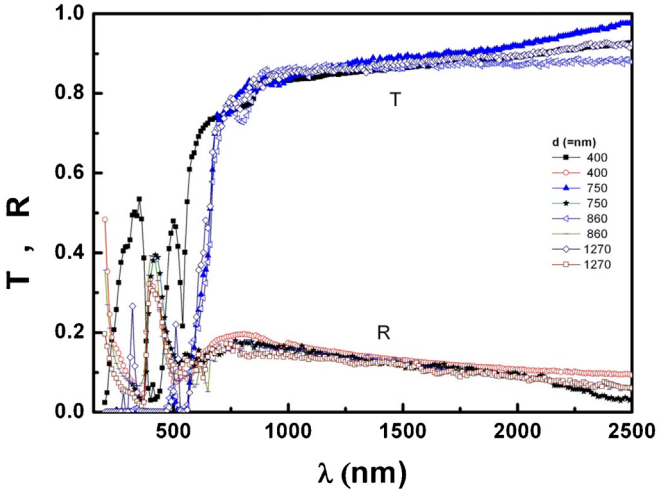

Fig. 4. The spectral dependence of the normal incidence transmittance, $T(\lambda)$ and reflectance, $R(\lambda)$ for CuTPP thin films.

3.2. Optical constants characteristics of CuTPP films

The spectral distribution of transmittance, $T(\lambda)$ and reflectance, $R(\lambda)$ spectra at normal incidence of light in the wavelength range 250–2500 nm for CuTPP thin films with different thickness ranging from 400 to 1270 nm are illustrated in Fig. 4. The spectra can be divided in two regions: (a) in the wavelength range <800 nm, the total sum of $T(\lambda)$ and $R(\lambda)$ is less than unity, implies the absorption existence and, (b) at wavelength greater than 800 nm, $T(\lambda)$ is much more greater than $R(\lambda)$ and their total sum is approximately equal to unity and then the films are transparent for light.

The values of $T(\lambda)$ and $R(\lambda)$ were used to determine the optical constants n and k by using Eqs. (2) and (3), respectively.

Refractive and extinction indices n and k of CuTPP films were determined from the measured transmittance and reflectance at normal light incidence with different thickness ranging from 400 to 1270 nm. The spectral dependences of both $n(\lambda)$ and $k(\lambda)$ are plotted in Fig. 5, taking into account the values used in the plots are the mean values of both $n(\lambda)$ and $k(\lambda)$ determined with considering the experimental errors in the calculations of n and k (~3% for n and 2.5% for k).This can be attributed to that both n and k are practically independent of film thickness in the desired thickness range. This behavior was recorded before by Farag and Yahia [4] and El-Nahass et al. [8].

The extinction index, k approaches minimum value at energy at 680 nm (1.82 eV). After which, k starts to increase again with increasing wavelength which is a characteristic feature of existence of free carriers [14].

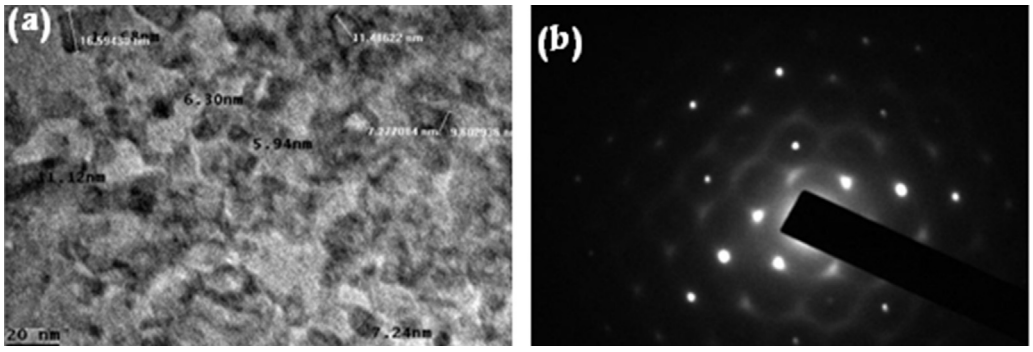

Fig. 3. TEM image for CuTPP as-deposited film: (a) selected area image at 200 kV and (b) selected area diffraction pattern of the same image.

Table 3
Discrete transition series (Q, B, N, M and L) observed in CuTPP compared with other organic corganic films.

Material	Q		B		N	M	L	O	References
CuTPP	1.38	2.3	3.0	–	4	5.1	5.92	–	Present work
NiTPP	1.95	2.38	2.98	3.27	4.13	4.77	5.1	–	[8]
CuPc	1.75	2.00	3.7	–	4.7	5.8	7.1	7.8	[17]
H_2Pc	1.82	2.02	3.8	–	4.3	6.0	7.0	7.6	[17]
ZnPc	1.72	2.00	3.7	–	4.3	5.9	6.8	7.6	[17]
CuPc-Cl	1.72	1.89	3.4	–	3.9	4.2	5.2	6.1	[17]

Refractive index of optical materials is considerably important for integrated optics devices, such as switches, filters and modulation applications and key parameter for the device design [4]. Refractive index, n of CuTPP thin film shows multipeaks due to multioscillation and can be explained by multioscillator model [15].

This anomalous behavior is due to the resonance effect between the incident electromagnetic radiation and the electron's polarization, which leads to the coupling of electrons in CuTPP films to the oscillating electric field [8].

3.3. Optical absorption characteristics of CuTPP films

The absorption coefficient, α, of CuTPP thin films is calculated by using the measured values of transmittance, $T(\lambda)$, and the reflectance, $R(\lambda)$. Fig. 6 shows the variation of absorption coefficient, α vs. $h\nu$ in UV–vis spectrum. The conjugated tetraphenyl porphyrin macrocycle with central copper atom shows high intense absorption (i.e. Soret band, appears at 3 eV [16]). The absorption peaks observed at 1.38 eV and 2.3 eV are labeled Q-band and extend with longer wavelengths with lower absorption. The other three bands labeled (N, M and L) appear in the UV region at 4 eV, 5.1 eV and 5.92 eV, respectively. All the discrete bands of CuTPP film are listed in Table 3 in comparison with other organic thin films [15,19]. The peaks of Q and B bands have generally interpreted in terms of π–π^* excitation between bonding and anti-bonding molecular orbitals [17]. The discrete transitions beyond the Soret band are intimately associated with the presence and character of the benzene rings on the CuTPP structure [19].

The strengths of these absorptions were reported to be about an order of magnitude less than the strength of the Soret transition, and each of their widths was observed to be more than twice that of the Soret band [8,17]. For these reasons it is possible that analogous transitions were present but could not be resolved in most of TPP derivative films spectra [17].

The band theory is applicable to describe the electronic transition in molecular organic systems [1,4,7–9]. Accordingly, for a molecular crystal, the valence band is formed by the combination of the highest occupied molecular orbital (HOMO; π-orbital) whereas the lowest unoccupied molecular orbital (LUMO; π^*-orbitals) contributes to the conduction band and separated by the band gap [1,4,7–9].

The analysis of optical absorption near the absorption band edge is a suitable method for determining the types of transitions and calculation of the optical band gap. The photon energy dependence of the interband absorption coefficient for direct or indirect allowed transitions (allowed or forbidden) can be expressed by the following equation [7,8]:

$$\alpha h\nu = B(h\nu - E_g)^r, \tag{5}$$

where $r = 1/2$ and $3/2$ for direct allowed and forbidden transitions, respectively, $r = 2$ and 3 for indirect allowed and forbidden transitions, respectively, and B is a characteristic constant, independent of the photon energy.

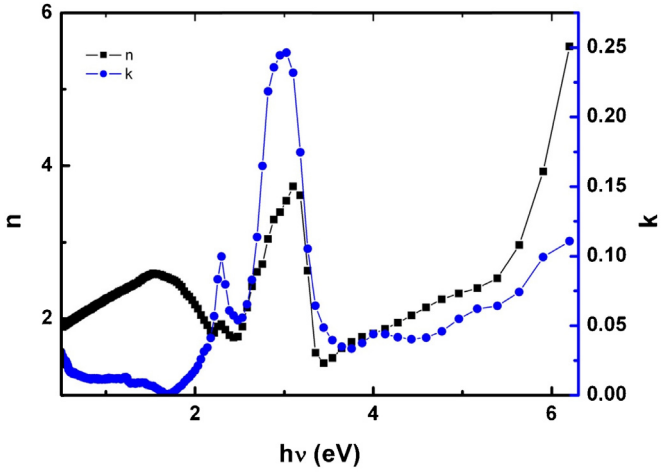

Fig. 5. Photon energy dependence of the mean values of real, n, and imaginary, k, parts of refractive index for CuTPP thin films.

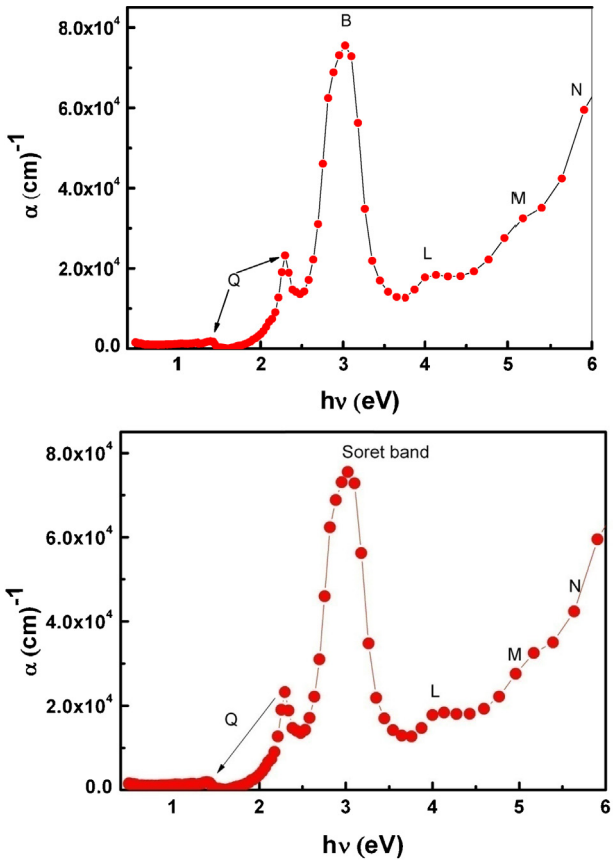

Fig. 6. Photon energy dependence of optical absorption coefficient, $\alpha(h\nu)$, of CuTPP thin films.

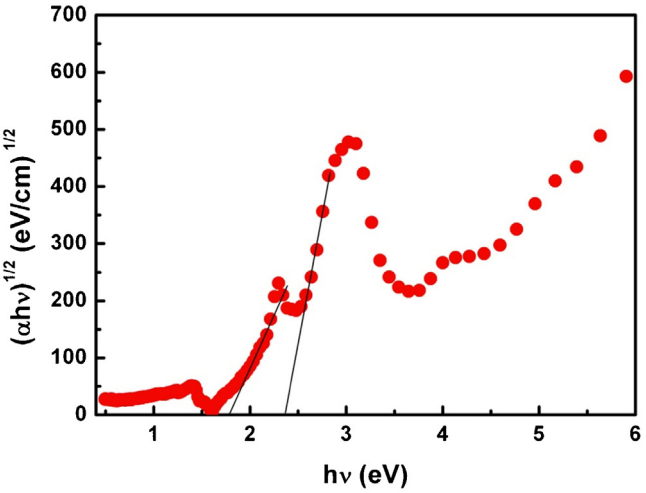

Fig. 7. Plot of $(\alpha h\nu)^{1/2}$ vs. $(h\nu)$ of CuTPP thin films.

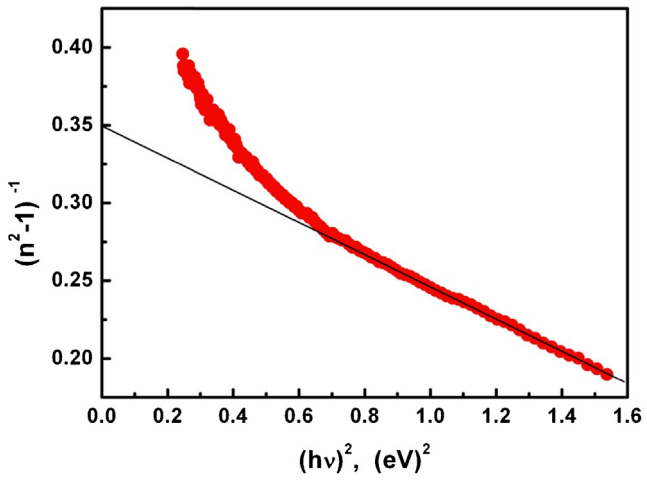

Fig. 8. Plot of $(n^2-1)^{-1}$ vs. $(h\nu)^2$ for CuTPP thin films.

Fig. 7 shows the photon energy dependence of $(\alpha h\nu)^{1/2}$ relation for the CuTPP thin films. The indirect band gap E_g can be evaluated from the x-axis intercepts at $(\alpha h\nu)^{1/2} = 0$.

According to Eq. (5), the values of the corresponding energies were found to be 1.93 and 2.88 eV. It should be noted that the first energy value is the onset optical gap E_{go} corresponds to the onset of optical absorption and formation of vacancies, interstitials Frenkel pairs or dislocations in the film microstructure [8]. The second energy value is the fundamental energy gap (energy gap between valence band "π-band" and conduction band "π*-band" [1,4]. Table 4 lists the determined energy gap of CuTPP compared with the previously obtained results for FeTPPCl [7], NiTPP [8] and CoMTPP [9]. As observed, most values of the energy gaps are comparable with each other and the small disagreement can be attributed to either the effect of central metal or the side groups of the organic materials.

3.4. Dispersion characteristics of CuTPP films

In the non-absorbing region, the refractive index, as a function of photon energy, can be analyzed on the basis of the single oscillator model, for photon energies below the interband absorption edge. The normal dispersion of refractive index has been analyzed by applying the single-oscillator model, expressed by Wemple and DiDomenico, is given by the following expression [7,8]:

$$(n^2-1)^{-1} = \frac{E_o}{E_d} - \frac{1}{E_o E_d}(h\nu)^2 \tag{6}$$

where E_d is the dispersion energy used to describe the dispersion of the refractive index and E_o is the single oscillator energy used to give quantitative information on the overall band structure of the material "average gap" [8].

The relation between $(n^2-1)^{-1}$ against $(h\nu)^2$ is shown in Fig. 8 for the average of different thickness in ranging from 400 to 1270 nm and fitting the data to a straight line, E_o and E_d can be determined from the intercept, E_o/E_d, and the slope, $-1/E_oE_d$. The oscillator energy E_o can be considered as an average energy gap and was found to be in proportion to the optical energy gap E_g, which agrees well with the relation $E_o \approx 1.22\,E_g$.

The calculated values of E_o and E_d as well as the corresponding high-frequency dielectric constant $(\varepsilon_\infty = n_\infty^2)$ for CuTPP films are tabulated in Table 5 in comparison with other related organic films.

As observed, most of dispersion parameters values are comparable with each other and the small disagreement can be attributed to either the effect of central metal or the side groups of the organic materials.

The relation between the real part of the dielectric constant ε_1 and wavelength (λ) is given by [7,8]:

$$\varepsilon_1 = n^2 = \varepsilon_L - \left(\frac{e^2}{4\pi^2 c^2 \varepsilon_0}\right)\left(\frac{N}{m^*}\right)\lambda^2 \tag{7}$$

where ε_0 is the permittivity of free space, ε_L is the lattice dielectric constant, c is the speed velocity and (N/m^*) is the ratio of free carrier concentration to its effective mass. The spectral distribution of the real dielectric constant, $\varepsilon_1 = n^2$, vs. λ^2 in the normal dispersion region, for CuTPP films is shown in Fig. 9. As observed, ε_1 decreases with increasing the square of the wavelength. For long wavelengths, the dependence of ε_1 on λ^2 is linear. The value of ε_L was obtained from the intercept of the experimental data point and the value of (N/m^*) can be calculated from the slope. The value of the lattice dielectric constant was determined by extrapolating the straight portion of the curve to intersect with the ordinate axis. The

Table 4
Energy gaps of CuTPP thin films compared with those for related organic films.

Material	E_{go} (eV)	E_{gF} (eV)	References
CuTPP	1.80	2.3	Present work
FeTPPCl	1.63	2.49	[7]
NiTPP	1.92	2.58	[8]
CoMTPP	1.53	3	[9]

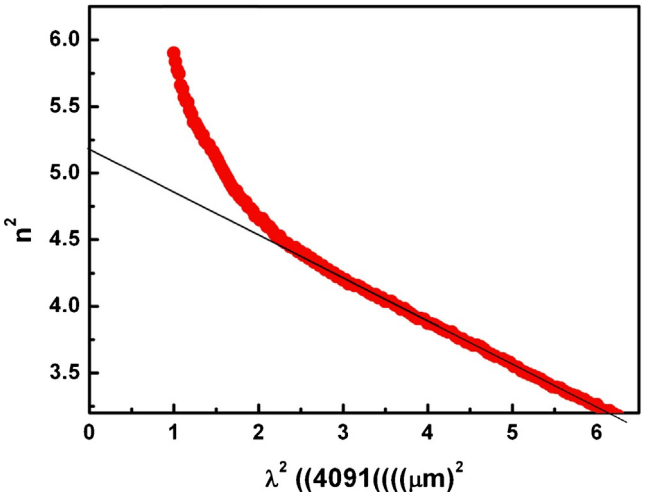

Fig. 9. Plot of n^2 vs. λ^2 of CuTPP thin films.

Table 5
Dispersion parameters of CuTPP thin films compared with other related organic films.

Material	E_o	E_d	ε_∞	ε_L	N/m^* (10^{46} g^{-1} cm^{-3})	$\chi^{(3)}$ (10^{-12} esu)	References
CuTPP	2.30	8.06	5.19	5.18	3.02	2.1	Present work
FeTPPCl	2.68	7.52	3.83	4.5	7.7	–	[7]
NiTPP	1.80	10.0	6.4	8.5	5.3	2.05	[8]
CoMTPP	3.02	7.99	3.65	4.07	9.82	–	[9]

values of ε_L and N/m^* are listed in Table 5 in comparison with those for some related organic films. Moreover, the proximity of $\varepsilon_L \sim \varepsilon_\infty$ gives an indication for the absence of free carrier contribution.

The dielectric properties are concerned with the storage and dissipation of electric and magnetic energy in materials [4]. The dielectric constant, $\tilde{\varepsilon}$ and its real, ε_1 and imaginary, ε_2, parts are described by the following relations [8]:

$$\tilde{\varepsilon}(h\nu) = \varepsilon_1(h\nu) + i\varepsilon_2(h\nu) \quad (8)$$

where

$$\varepsilon_1 = (n^2 - k^2) \quad (9)$$

and

$$\varepsilon_2 = 2nk \quad (10)$$

The photon energy dependencies of ε_1 and ε_2 for the average thickness of CuTPP thin films is shown in Fig. 10. As observed, the real and imaginary parts follow the same pattern and the values of the real part are higher than the imaginary part. Moreover, the variation of the dielectric constant vs. photon energy indicates that some interactions between photons and electrons in the film are produced in this energy range which observed on the shapes of ε_1 and ε_2 and they cause formation of peaks in the dielectric spectra [4,7,8].

Volume energy loss function (VELF) and surface energy loss function (SELF) are quantities of interest in studying the rate of energy loss of high energy electrons passing through material and can be calculated by using the following expressions [4,8].

$$VELF = \frac{\varepsilon_2}{\varepsilon_1^2 - \varepsilon_2^2} \quad (11)$$

$$SELF = \frac{\varepsilon_2}{(\varepsilon_1 + 1)^2 + \varepsilon_2^2} \quad (12)$$

Fig. 11 shows the photon energy dependence of the volume and surface energy loss functions for the average thickness of CuTPP thin films.

The figure indicate that the energy loss by the free charge carriers when traversing through the bulk material has approximately the same behavior as when they traverse the surface in particular for relativity lower energies [9]. Moreover, it is also clear that there is no significant difference between them at lower and higher photon energies but the VELF increases more than SELF at the particular peaks which characterized the CuTPP film.

The complex optical conductivity, σ, is related to the complex dielectric constant, by $\sigma = \sigma_1 + i\sigma_2$ (where $\sigma_1 = \omega\varepsilon_2\varepsilon_0$ and $\sigma_2 = \omega\varepsilon_1\varepsilon_0$) [4]. The real, σ_1 and imaginary, σ_2 parts of the optical conductivity dependence of photon energy are shown in Fig. 12. It is seen that the optical conductivity increases with the increase of photon energy in the higher energy range ($h\nu > 3.5$ eV). Dongol et al. [6] suggested that the increase of the optical conductivity is due to electrons excited by incident photon energy and the origin of this increasing may be attributed to some changes in the film structure which caused by the charge ordering effect. Optical conductivity curves are always characterized by two maxima, which correspond approximately to both the onset optical gap, E_{go}, and the fundamental energy gap, E_{gF}.

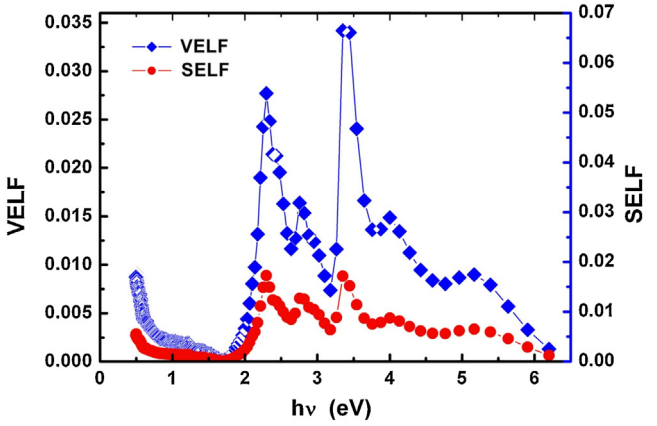

Fig. 11. Photon energy dependence of VELF and SELF of CuTPP thin films.

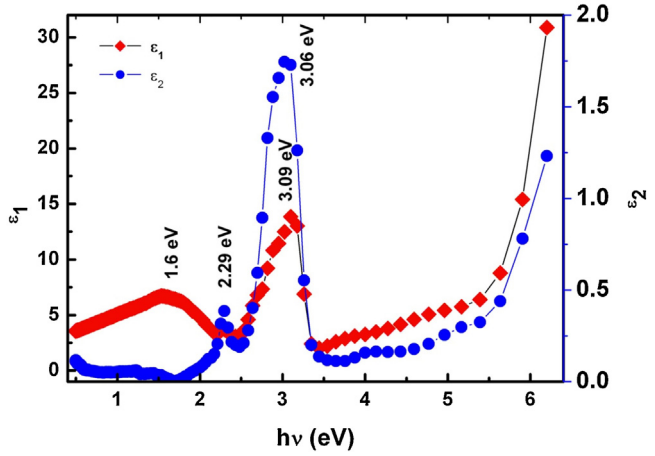

Fig. 10. Photon energy dependence of ε_1, ε_2 of CuTPP thin films.

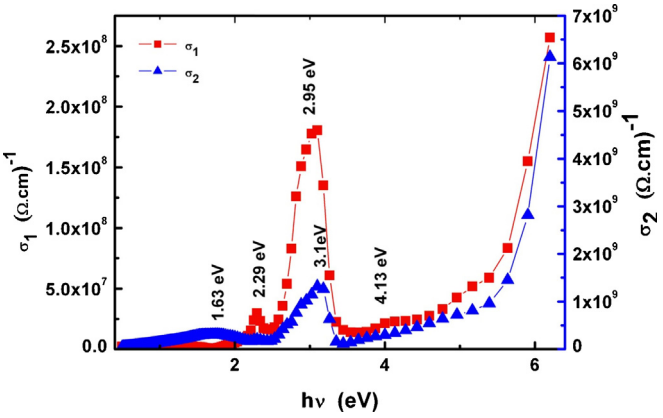

Fig. 12. Photon energy dependence of σ_1 and σ_2 of CuTPP thin films.

3.5. Nonlinear optical characteristics of CuTPP films

Nonlinear optics is the branch of optics that describes the behavior of light in nonlinear media, that is, media in which the dielectric polarization, P, response nonlinearly to the electric field, E, of the light [18].

The non-linear optical response to an applied optical wave can be described as [19].

$$p(t) = \chi^{(1)}E(t) + \chi^{(2)}E^2(t) + \chi^{(3)}E^3(t) + \cdots \quad (13)$$

where the coefficients $\chi(n)$ are the nth order susceptibilities of the medium and the presence of such a term is generally referred to as an nth order nonlinearity.

Third-order nonlinear optical effects, $\chi^{(3)}$, are the important basis of a number of applications such as high capacity communication networks [20]. Third order susceptibility have been studied experimentally in a large variety of materials as homogenous bulk glasses, nano material, polymers and semiconductor or glasses doped with either semiconductors [21].

El-Nahass [8] stated that one of the main property of the tetrapyrrole derivatives is their great third-order optical nonlinearity that attributed to their highly polarizable extended two-dimensional π-electron system.

From Miller's generalized rule [22], the nonlinear susceptibility, $\chi^{(3)}$, can be calculated according to the following expression:

$$\chi^{(3)} = \frac{A(n_o^2 - 1)^4}{(4\pi)^4}, \quad (14)$$

where A is a frequency independent quantity and nearly the same for all materials, $A \approx 1.7 \times 10^{-10}$ esu [8] and $n \to n_o$ when $h\nu \to 0$. Values of the third order nonlinear optical susceptibility are anticipated to be a base for the production of all high-frequency ultrafast optical switches and photonic devices [23]. The value of $\chi^{(3)}$ for the average thickness of CuTPP thin film as listed in Table 5 in comparison with that for NiTPP thin film [8]. As observed, a good agreement for the obtained value of $\chi^{(3)}$ which gives evidence for the applicability of the nonlinear characteristics of CuTPP films.

4. Conclusion

In this work, CuTPP thin films were synthesized by using conventional thermal evaporation and the prepared films are characterized as good adherent and nearly homogeneous film. The XRD obtained for CuTPP films confirms that the material is nanocrystalline with average crystallite size of 60 nm by using modified Scherrer's formula.

The absorption bands in UV–vis region are generally interpreted in terms of π to π* transitions between bonding and antibonding molecular orbital. The optical constants of CuTPP were calculated and fond to be independent of film thickness in the thickness range (400–1275 nm). The allowed transitions were found to be indirect transitions. An interpretation of single oscillator model has been described for the analysis of refractive index dispersion in the transparent region. Photon energy distribution for dispersion parameters such as ε_1, ε_2, *VELF*, *SELF*, $\sigma_1(\omega)$ and $\sigma_2(\omega)$ are estimated. The third-order nonlinear susceptibility was also estimated.

References

[1] A.A.M. Farag, W.G. Osiris, E.A.A. El-Shazly, J. Alloys Compd. 509 (2011) 6467–6475.
[2] A.S. Kavasoglu, F. Yakuphanoglu, N. Kavasoglu, O. Pakma, O. Birgi, S. Oktik, J. Alloys Compd. 492 (2010) 421.
[3] S. Rasouli, S.J. Moeen, J. Alloys Compd. 509 (2011) 1915.
[4] A.A.M. Farag, I.S. Yahia, Synth. Met. 161 (2011) 32.
[5] Available from: http://goldbook.iupac.org/PDF/C01267.pdf
[6] M. Dongol, M.M. El-Nahass, A. El-Denglawey, A.F. Elhady, A.A. Abuelwafa, Curr. Appl. Phys. 12 (2012) 1178–1184.
[7] M.M. El-Nahass, A.F. El-Deeb, H.S. Metwally, H.E.A. El-Sayed, A.M. Hassanien, Solid State Sci. 12 (2010) 552.
[8] M.M. El-Nahass, H.M. Abd El-Khalek, A.M. Nawar, Eur. Phys. J.: Appl. Phys. 57 (2012) 30201.
[9] M.M. El-Nahass, A.H. Ammar, A.A. Atta, A.A.M. Farag, E.F.M. El-Zaidia, Opt. Commun. 284 (2011) 2259.
[10] J. Spadavecchia, R. Rella, P. Siciliano, M.G. Manera, A. Alimelli, R. Paolesse, C. Di Natale, A. D'Amico, Sens. Actuators B 115 (2006) 12.
[11] G. Laukaitish, S. Lindroos, S. Tamulevicius, M. Leskela, M. Rackaitis, Appl. Surf. Sci. 161 (2000) 396–405.
[12] M.M. El-Nahass, A.A.M. Farag, F.S.H. Abu-Samaha, E. Elesh, Vacuum 99 (2014) 153–159.
[13] M. Abdel Rafea, H. Farid, Mater. Chem. Phys. 113 (2009) 868.
[14] H.M. Zeyada, M.M. EL-Nahass, I.S. Elashmawi, A.A. Habashi, J. Non-Cryst. Solids 358 (2012) 625–636.
[15] M.M. El-Nahass, A.M. Farag, K.F. Abd El-Rahman, A.A.A. Darwish, Opt. Laser Technol. 37 (2000) 513–523.
[16] W.R. Scheidt, Y.J. Lee, Struct. Bond. (Berlin) 1 (1987) 64.
[17] B.H. Schechtman, W.E. Spicer, J. Mol. Spectrosc. 33 (1970) 28.
[18] R.W. Boyd, G.L. Fischer, Encyclopedia of Materials: Science and Technology, 2001, pp. 623.
[19] D. Cotter, R. Manning, K. Blow, A. Ellis, A. Kelly, D. Nesset, I.S. Phillip, A. Poustie, D. Rogers, Nonlinear Opt. 286 (1999) 1528.
[20] G. Banfi, V. Degiorgio, D. Ricard, Adv. Phys. 47 (1998) 510.
[21] J.J. Wyne, Phys. Rev. 178 (1969) 1295.
[22] R.C. Miller, Appl. Phys. Lett. 5 (1964) 17.
[23] M.C. Gupta, Handbook of Photonics, CRC Press, Boca Raton, FL, 1997.